Electronic Supplementary Material (ESI) for Journal of Materials Chemistry A.

Supplementary Information For

Solar-driven valorisation of glycerol on $BiVO_4$ photoanodes: effect of co-catalyst and reaction media on reaction selectivity

Yi-Hsuan Wu,[a] Denis A. Kuznetsov,[a] Nicholas C. Pflug,[b] Alexey Fedorov,[a] and Christoph R. Müller*[a]*

[a] *Department of Mechanical and Process Engineering, Leonhardstrasse 21, ETH Zürich, 8092 Zürich, Switzerland*

E-mail: denisk@ethz.ch; muelchri@ethz.ch

[b] *Department of Environmental Systems Science, ETH Zürich, Universitätstrasse 16, 8092 Zurich, Switzerland*

Table of Content

Experimental Procedures

Materials

Bismuth nitrate pentahydrate ($Bi(NO_3)_3 \cdot 5H_2O$, 98%, Sigma-Aldrich), potassium iodide (KI, 99%, Sigma-Aldrich), p-benzoquinone (98%, Sigma-Aldrich), vanadyl acetylacetonate ($VO(acac)_2$, ≥ 97 %, Sigma-Aldrich), sodium tungstate dihydrate ($NaWO_4 \cdot 2H_2O$, 99%, Sigma-Aldrich), nitric acid solution (HNO_3, 70%), ethanol absolute (EtOH), boric acid (H_3BO_3, ≥ 99.5 %, Fisher), potassium hydroxide (KOH, ca. 85%, Acros), hydrogen peroxide solution (H_2O_2, 35%, Sigma Aldrich), deuterium oxide (D_2O, 99.9 at % D, Sigma-Aldrich) and dimethyl sulfoxide (DMSO, ≥ 99.9 % (GC), Sigma-Aldrich) were purchased from the respective vendor and used as received.

All chemicals were stored under ambient conditions, except DMSO that was kept in the glovebox. Milli-Q water (18.2 MΩ·cm) was used to prepare solutions. Fluorine-doped tin oxide (FTO) coated glass were purchased from Xop Glass (TEC-15). For electrolyte preparation, H_3BO_3, KOH, or H_2O_2 solutions were used.

Reference chemicals, i.e. dihydroxyacetone, D-(+)-glyceraldehyde, glycolic acid (99 %), D-glyceric acid calcium salt dihydrate (99 %), lithium beta-hydroxypyruvate hydrate (≥ 97 %), oxalic acid (≥ 99 %), tartronic acid (≥ 97 %), sodium mesoxalate monohydrate (≥ 98 %), glycolaldehyde dimer, glyoxylic acid monohydrate (98 %), formic acid (≥ 95 %), and formaldehyde (37 wt% in water) were purchased from Sigma-Aldrich.

Fabrication of $BiVO_4$ photoanodes

$BiVO_4$ photoanodes were synthesized via a modified literature procedure.[1, 2] An aqueous solution (150 ml) containing KI (400 mM) and $Bi(NO_3)_3$ (15 mM) was prepared and stirred for 20 min. Several drops of HNO_3 was then added to adjust the pH to 1.8 ± 0.05, and the orange blurry solution turned transparent. Ethanol solution of p-benzoquinone (5 mM, 60 ml) was then added drop wise into the as-prepared solution, and pH was adjusted to 3.4 ± 0.05 with HNO_3.

The electrodeposition of BiOI was carried out in a conventional three-electrode cell with FTO as a working electrode, Ag/AgCl (saturated) and platinum mesh as reference and counter electrodes, respectively. Two-step potentiostatic electrodeposition was employed. First, the working electrode was held at −0.48 V vs. Ag/AgCl for 20 s and then at −0.2 V vs. Ag/AgCl for 10 min. The as-deposited BiOI was washed with DI-water, dried at room temperature and stored in air.

To convert BiOI to $BiVO_4$, 60 µL of $VO(acac)_2$ solution in DMSO (200 mM, 10 ml) was drop cast on each electrode (ca. 1.8 cm^2), then the electrodes were calcined in air at 450 ºC for 2 h (2 ºC min^{-1}). To fabricate W:$BiVO_4$ electrodes, various concentrations of sodium tungstate were added to $VO(acac)_2$ solution and stirred for 1 h. The optimized W/V molar ratio is 0.036 (3.6 % W added to the solution of $VO(acac)_2$, **Figure S1**). To remove the excess of V_2O_5 from the electrode surface after the calcination step, electrodes were immersed in aqueous 1.0 M KOH and held for 20 min. For chronoamperometric glycerol oxidation, the electrode area was controlled as ca. 3.6 cm^2 where the volume of W-/V-containing solution was 120 µL.

Atomic Layer Deposition

Deposition of the $NiO_x(OH)_y$ films was performed on a commercial ALD system (Sunale R-150B, Picosun). The electrodes were place horizontally on a Si wafer and were exposed to alternating pulses of bis(cyclopentadienyl)nickel (Cp_2Ni, 99%, Strem Chemicals) and DI water. One ALD cycle contained

consecutive pulses of Cp_2Ni and water (durations were 2.0 and 0.1 s, respectively, both at 250 °C deposition temperature). Overall, 50 ALD cycles was performed. Nitrogen was used as purge (15 s purge duration) and carrier gas.

Materials Characterization

X-ray diffraction patterns were acquired by PANalytical Empyrean X-ray Powder Diffractometer with Cu Kα radiation (λ =1.5418 Å, 40 mA, and 40 kV). Samples were measured in the 2θ range of 10–70° using a step size of 0.02° with a time duration of 140 s per step.

Inductively coupled plasma optical emission spectrometry (ICP-OES) measurements were performed using Agilent 5100 VDV.

Transmission electron microscopy (TEM) imaging was performed on a FEI Talos F200X microscope equipped with a high-brightness field-emission gun, a high-angle annular dark field (HAADF) detector, and a large collection-angle EDX detector. The operation voltage was 200 kV in scanning transmission electron microscopy (STEM) mode.

The X-ray photoelectron spectroscopy (XPS) measurements were conducted on a Sigma 2 instrument (Thermo Fisher Scientific) equipped with a UHV chamber (non-monochromatic 200 W Al Kα source, a hemispherical analyzer, and a seven-channel electron multiplier). Pass energy of 20 eV and 25 eV was set for the survey and the narrow scans, respectively. The position of the C 1s peak (284.8 eV) was used to calibrate the XPS binding-energy scale for all materials.

(Photo)electrochemical Measurements

All (photo)electrochemical measurements were performed using VoltaLab 40 potentiostat in ambient environment under illumination with LOT-Oriel solar simulator setup (150 W Xe arc lamp combined with an AM 1.5 G filter) in a conventional three-electrode system. The intensity of light was adjusted to 100 mW cm^{-2} before each measurement. All PEC experiments were carried out in a customized glass cell with aperture area of around 2.8 cm^2. The recorded potentials (V vs. Ag/AgCl) were converted to reversible hydrogen electrode (RHE) scale by applying the Nernst equation ($V_{RHE} = V_{Ag/AgCl} + 0.1976 + 0.059 \times pH$). The electrolytes used were 0.1 M glycerol in 0.5 M Na_2SO_4 (pH $\approx$ 6.8) or 0.5 M potassium borate buffer (KB_i, pH = 9.3). For sulfite oxidation, electrolyte of 0.1 M Na_2SO_3 in 0.5 M KB_i was prepared. The linear scan voltammetry (LSV) measurements were conducted at scan rate of 10 mV s^{-1}.

Continuous (10 h) glycerol oxidation were performed at potentials of 0.8 V_{RHE} or 1.2 V_{RHE} under illumination for all electrodes, while chopped chronoamperometry experiment was carried out at 0.3 V_{RHE}, 0.5 V_{RHE}, and 0.8 V_{RHE}. A two-compartment cell with an anion-exchange membrane (fumasep FKB-PK-130, FuMA-Tech) was used to avoid simultaneous reduction of oxidized products at the cathode. In continuous glycerol-oxidation-reaction (GOR) experiment, the volume of anode compartment was 33 ml. After 5 h and 10 h, aliquots of reaction mixture (1.5 ml) were withdrawn for high-performance liquid chromatography (HPLC) analysis. Additional 2 ml of post-reaction electrolyte was collected for nuclear magnetic resonance (NMR) analysis. Prior to analysis, samples were kept in a fridge (*ca*. 4 °C).

Calculation of Hole Efficiency

Photoelectrochemical activity toward reduced reagents in electrolyte directly reflect on the photocurrent (J_{ph}). Photocurrent of a material is generally seen as dominated by three factors: current density where sunlight influx is harvested without reflection (J_{abs}), the separation efficiency of photo-generated charge carriers (η_{sep}), and charge injection efficiency (η_{inj}).

$$J_{ph} = J_{abs} \times \eta_{sep} \times \eta_{inj} \quad (1)$$

As the kinetics of sulfite oxidation (SOR) are significantly faster than that of water oxidation, η_{inj} is set as 100 %. When using the same electrode, J_{abs} and η_{sep} are identical for water, glycerol, or sulfite oxidation. As a result, the only difference between the photocurrents of OER, GOR, and SOR lies in η_{inj}. Since the concentration of glycerol in this study is 0.1 M, the concentration of sulfite is thus kept 0.1 M. The hole injection efficiency for OER and GOR can be obtained through

$$\eta_{inj}^{Water} = \frac{J_{ph}^{OER}}{J_{ph}^{SOR}} \quad (2)$$

$$\eta_{inj}^{Glycerol} = \frac{J_{ph}^{GOR}}{J_{ph}^{SOR}} \quad (3)$$

Chromatographic Determination of Products

The samples collected after chronoamperometry experiments were analyzed by HPLC (Waters 2695 separation module coupled with a refractive index detector). Columns used were Aminex HPX 87-H (Bio-Rad) or Agilent Hi-Plex H (7.7 × 300 mm, 8-µm). Diluted sulfuric acid (0.005 M) was employed as eluent. Injection volume per sample was 20 µl with the system flow rate of 0.5 ml min^{-1} and column temperature set to 60 °C. HPLC data was collected for 20 min, which exceeds the retention time of all chemicals in this study.

Product Analysis by NMR

^{1}H NMR, ^{13}C NMR, and heteronuclear single quantum coherence (HSQC) data were recorded using a Bruker AVANCE III-400 spectrometer (400 MHz) using D_2O as the solvent at 298 K. The samples were first dried in a vacuum oven at 298 K (4 h), then dissolved in D_2O. Chemical shift of the HOD peak (δ = 4.80 ppm) in ^{1}H NMR spectra was used for calibration. Number of scans to collect ^{13}C spectra was 8192. All NMR data were processed using Bruker Topspin 4.0.8 software.

Quantification of Products from Continuous Glycerol Oxidation

(1) Production rate (per unit area) of a specific compound (e.g. GALD) was calculated as follows:

$$r = \frac{C_{GALD} \times V_{anode}}{t \times A_{anode}}$$

where C is the measured concentration of the compound (mM), V_{anode} is the electrolyte volume of the anode compartment (L), t is the reaction time (h), and A_{anode} is the reaction area of the anode (area under exposure, m^2).

(2) Faradaic efficiency for converting glycerol to a compound should be calculated by
(i) employing the stoichiometry balance between reagents and products. Here we take GALD, GCALD, and FA as examples:

$1\ C_3H_5(OH)_3 + 3\ H_2O \rightarrow 1\ C_3H_4(OH)_2O + 2\ H^+ + 2\ e^-$ $\quad n_{GALD} = 2\ e^-$

$2\ C_3H_5(OH)_3 \rightarrow 3\ C_2H_4O_2 + 4\ H^+ + 4\ e^-$ $\quad n_{GCALD} = \frac{4}{3}\ e^-$

$1\ C_3H_5(OH)_3 + 3\ H_2O \rightarrow 3\ CH_2O_2 + 8\ H^+ + 8\ e^-$ $\quad n_{FA} = \frac{8}{3}\ e^-$

where *n* means number of holes (electrons) to transform glycerol into a specific compound.

(ii) then compare the total charge transfer with the required charge per mole of product.
The total number of moles of holes (electrons) measured during the reaction period is:

$$e_{input} = \frac{Q}{F}$$

where Q is the charge transfer (C), calculated by the measured, I (A), times sampling time, t (s); F is the Faraday constant (96485 C mol^{-1})

The Faradaic efficiency can be interpreted as the determined number of the product (mmol) divided by the total charge transfer (mmol e^-). Here we take GALD for instance:

$$FE_{GALD} = \frac{Number\ of\ holes\ to\ oxidize\ glycerol\ to\ generated\ GALD}{Number\ of\ holes\ collected\ (e_{input})} \times 100\ \%$$

$$= \frac{n_{GALD} \times C_{GALD} \times V_{Anode}}{e_{input}} \times 100\ \%$$

$$= \frac{e_{output}}{e_{input}} \times 100\ \%$$

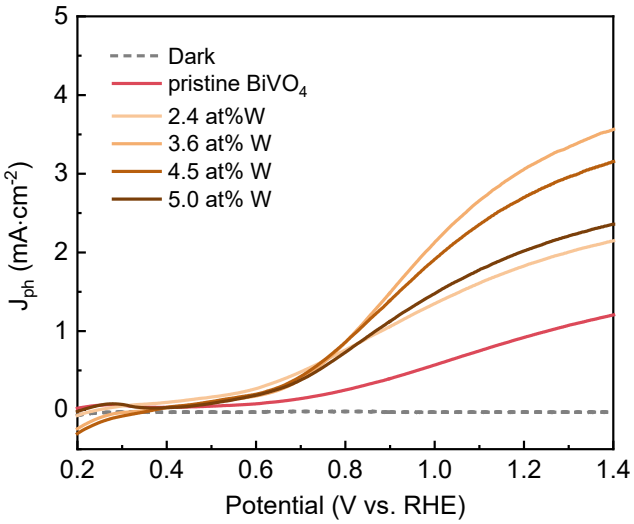

Figure S1 Linear sweep voltammetry of pristine $BiVO_4$ and W:$BiVO_4$ at different W/V ratios taken in synthesis, i.e. $NaWO_4$/$VO(acac)_2$. The actual W content in as-synthesized W:$BiVO_4$ films discussed in the main text (3.6 at% W) is 0.5 at% as followed from ICP analysis. The electrolyte was 1.0 M KB_i (pH = 9.3). Scan rate: 10 mV s^{-1}.

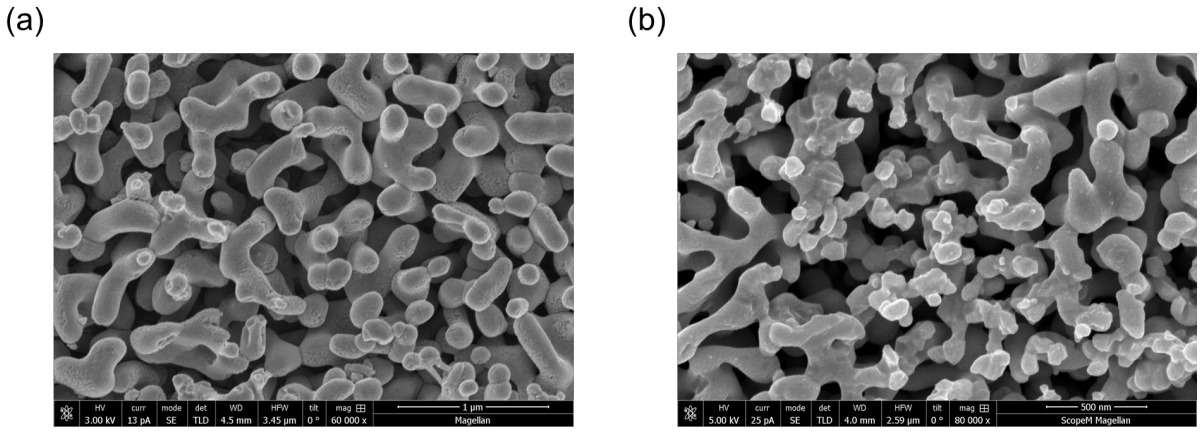

Figure S2 SEM images of (a) W:$BiVO_4$ and (b) $NiO_x(OH)_y$/W:$BiVO_4$.

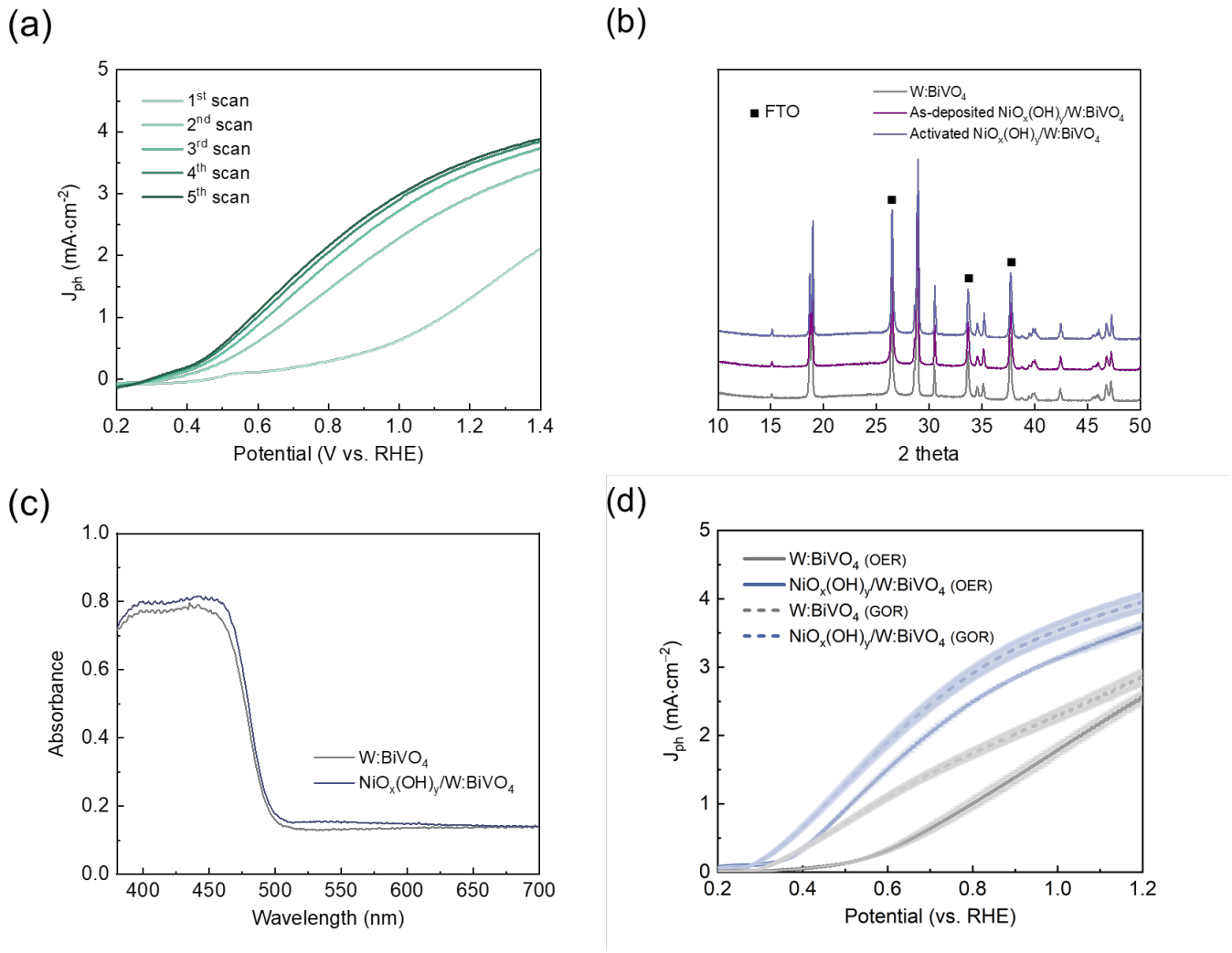

Figure S3 (a) Linear sweep voltammetry of $NiO_x(OH)_y$/W:$BiVO_4$ under anodic activation in 0.5 M KB_i. (b) XRD patterns of W:$BiVO_4$, as-deposited $NiO_x(OH)_y$/W:$BiVO_4$, and activated $NiO_x(OH)_y$/W:$BiVO_4$. (c) Absorption spectra of W:$BiVO_4$ and $NiO_x(OH)_y$/W:$BiVO_4$. (d) Averaged linear sweep voltammetry of W:$BiVO_4$ and $NiO_x(OH)_y$/W:$BiVO_4$ in 0.5 M KB_i with and without 0.1 M glycerol. Scan rate: 10 mV s^{-1}.

Table S1 Binding energies for O 1s components and Ni 2p components of as-deposited and anodically activated $NiO_x(OH)_y$ catalysts on W:$BiVO_4$ electrodes.

Ni 2p		Composition (%)		O 1s		Composition (%)	
		As-deposited	Anodically activated			As-deposited	Anodically activated
Ni^0	852.9 eV	5	3	**O_L**	529.5 eV	73	22.5
Ni^+	854.7 eV	28	9	**O_V**	531.4 eV	21	22
Ni^{2+}	855.7 eV	42	52	**O_{surf}**	532.2 eV	2	41.5
Ni^{3+}	856.9 eV	25	36	**O_{adv}**	533.5 eV	4	14

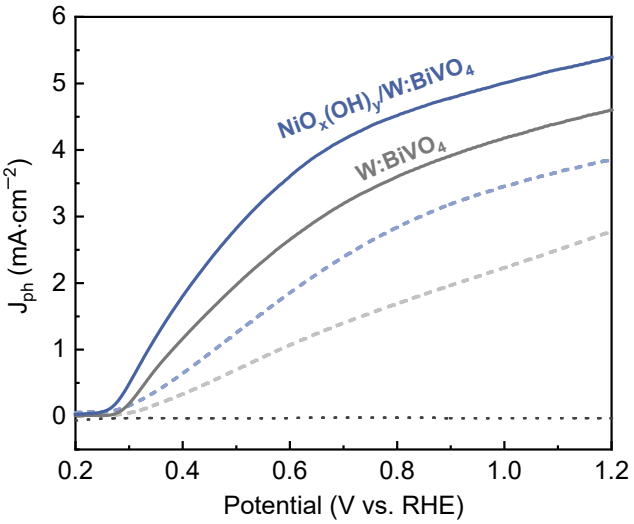

Figure S4 Linear sweep voltammetry of W:$BiVO_4$ and $NiO_x(OH)_y$/W:$BiVO_4$ for sulfite oxidation (solid curve) and glycerol oxidation (dashed curve) in 0.5 M KB_i. Concentration of both Na_2SO_3 and glycerol was 0.1 M. Scan rate = 10 mV s^{-1}.

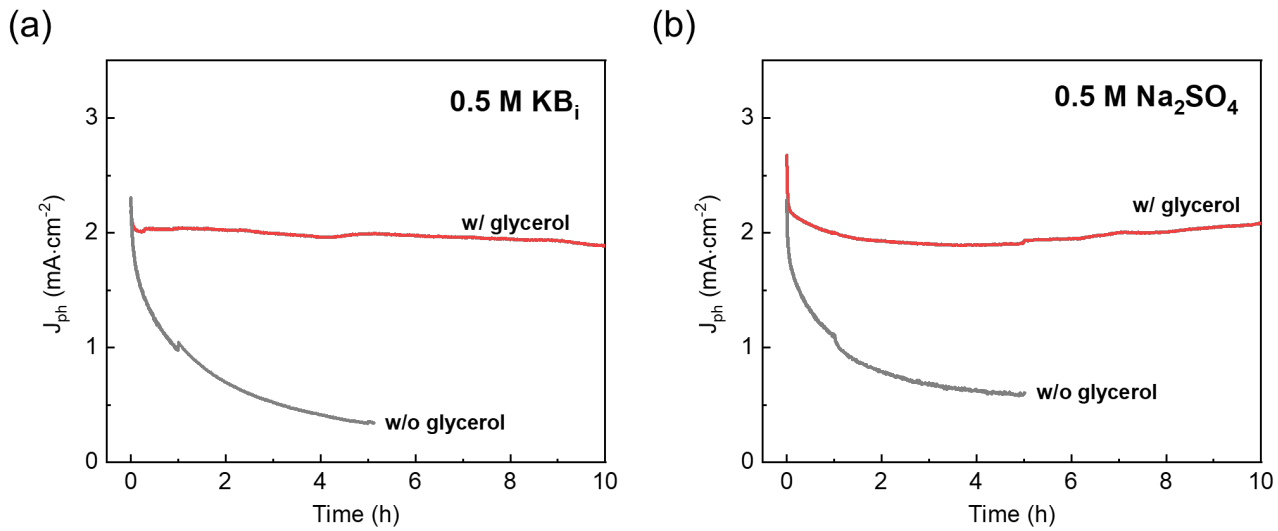

Figure S5 Photo-assisted chronoamperometry plots at 1.2 V_{RHE} using W:$BiVO_4$ as the photoanode in (a) 0.5 M KB_i and (b) 0.5 M Na_2SO_4 with and without 0.1 M glycerol. Reactions under AM 1.5 G, 100 mW cm^{-2} illumination.

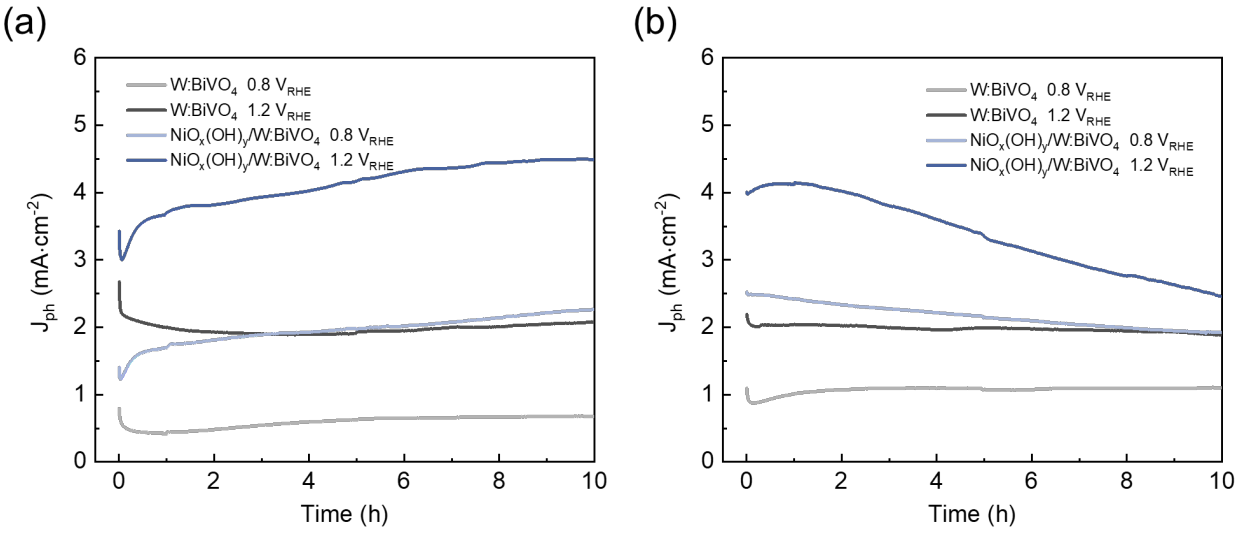

Figure S6 10-h chronoamperometry glycerol oxidation at different bias under AM 1.5 G, 1 Sun illumination on both W:$BiVO_4$ and $NiO_x(OH)_y$/W:$BiVO_4$ in (a) 0.5 M Na_2SO_4 and in (b) 0.5 M KB_i; both with the addition of 0.1 M glycerol.

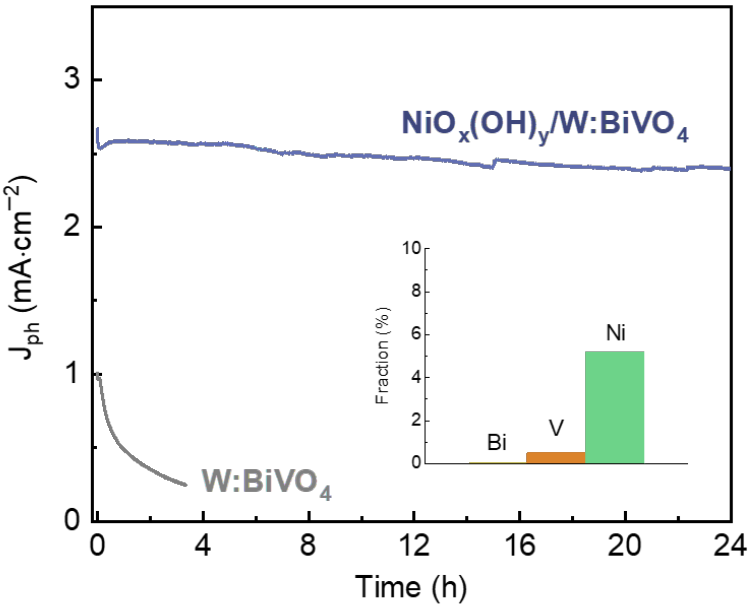

Figure S7. Chronoamperometry test for $W:BiVO_4$ and $NiO_x(OH)_y/W:BiVO_4$ at 0.8 V_{RHE} in 0.5 M KB_i under AM 1.5 G, 1 Sun illumination. The inset shows the fraction of dissolved elements in the post-reaction electrolyte solution (24 h of electrolysis) as followed from ICP measurements.

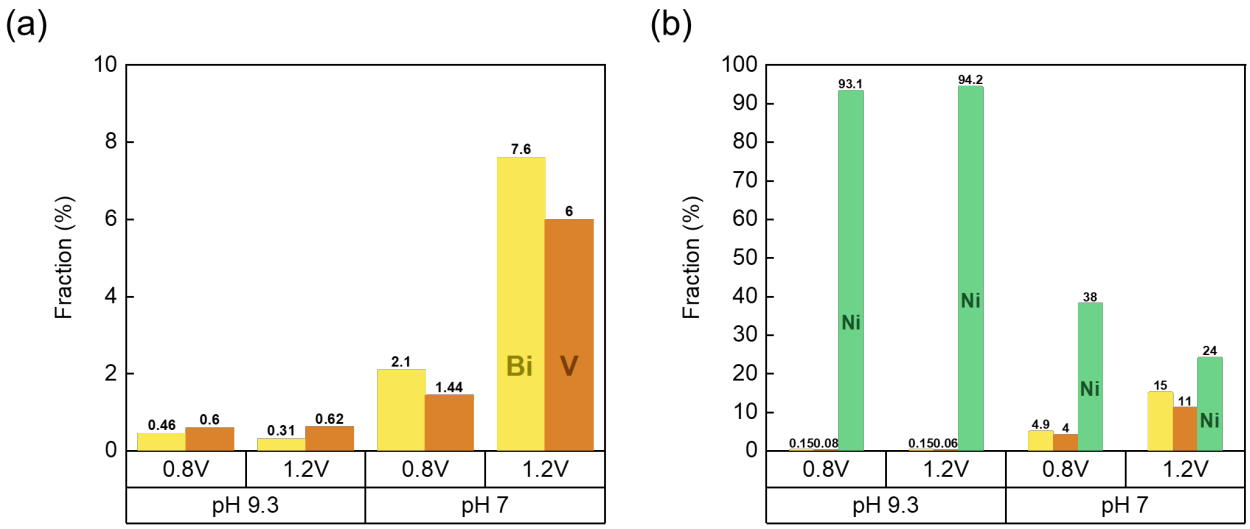

Figure S8 Fraction of dissolved elements from (a) W:$BiVO_4$ and (b) $NiO_x(OH)_y$/W:$BiVO_4$ in the post-reaction electrolyte after a 10-h potential static glycerol oxidation in different pH environments and at different applied bias. Results were acquired from ICP measurements.

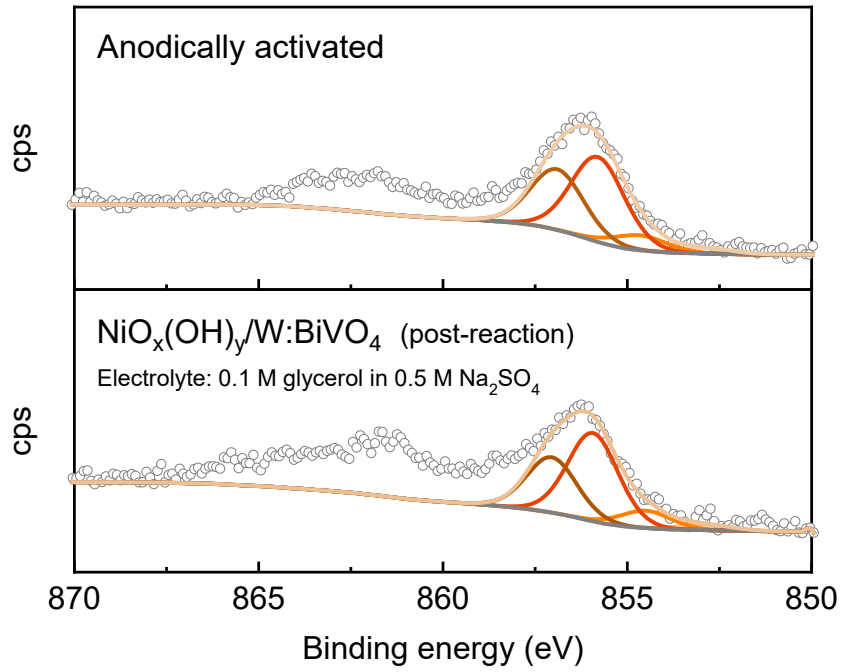

Figure S9 Ni 2p core level XPS of the anodically activated $NiO_x(OH)_y$/$BiVO_4$ electrode before and after the chronoamperometric glycerol oxidation (0.5 M Na_2SO_4, 1.2 V_{RHE}, 10 h).

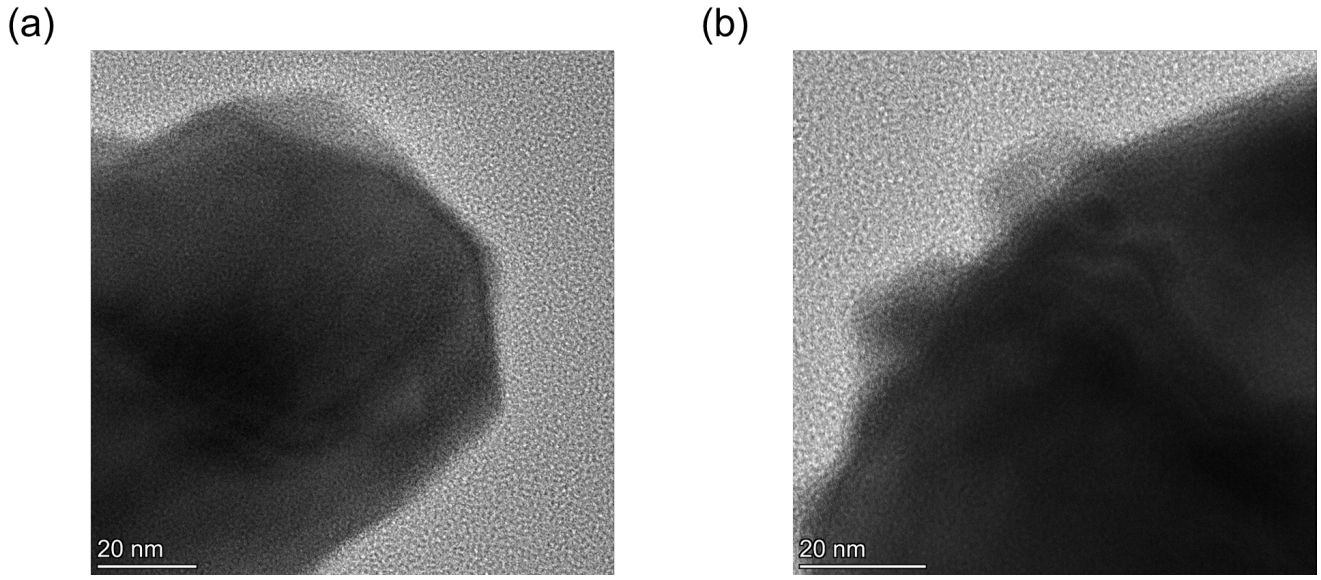

Figure S10 Morphology characterization by HRTEM of post-GOR (a) W:$BiVO_4$ and (b) $NiO_x(OH)_y$/W:$BiVO_4$ electrodes after 10 h potential static glycerol oxidation in 0.5 M KB_i at 1.2 V_{RHE}.

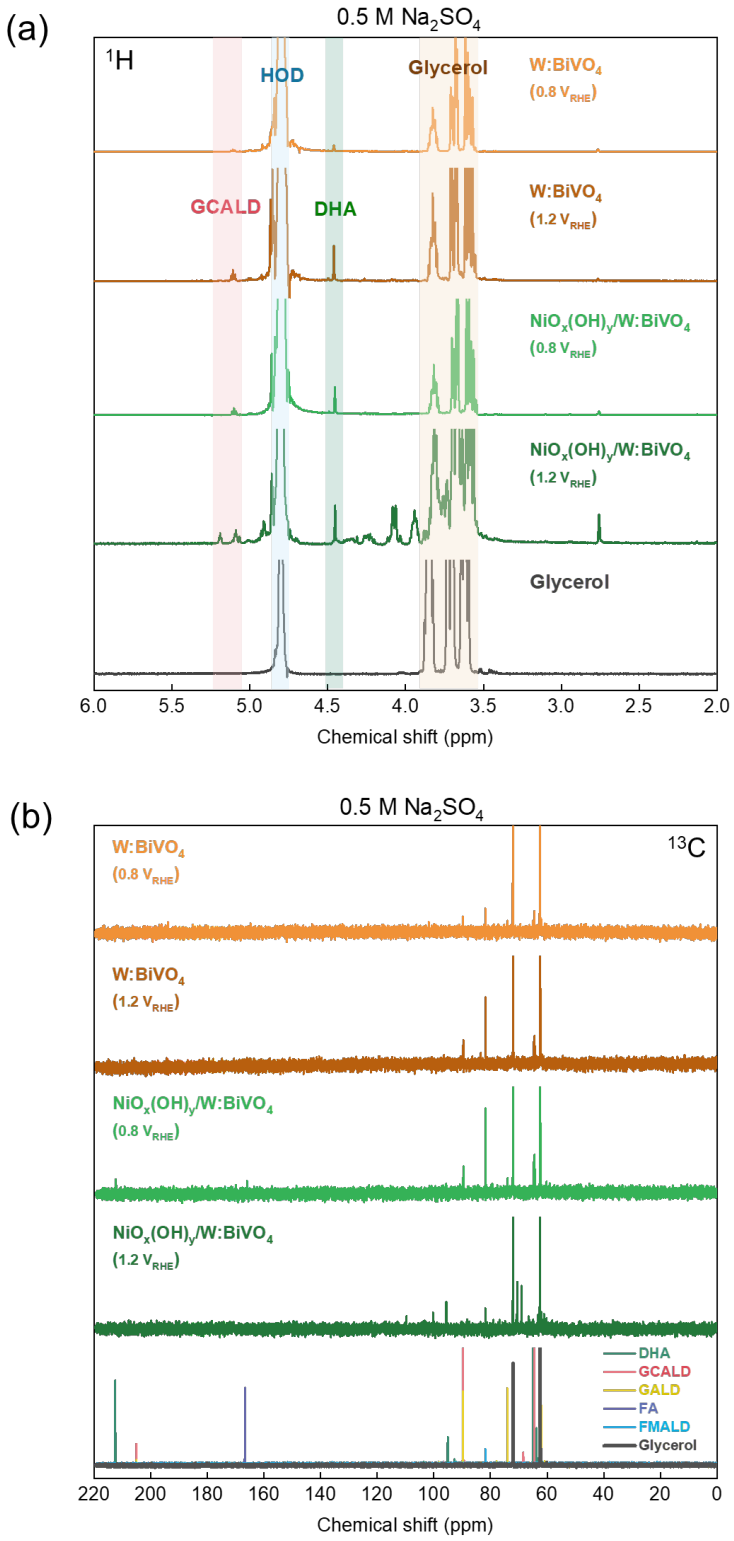

Figure S11 ^{1}H (a) and ^{13}C NMR (b) spectra (400 and 100 MHz, respectively, D_2O) of the reaction mixture of 0.1 M glycerol in 0.5 M Na_2SO_4 after 10 h constant potential (0.8 V_{RHE}/1.2 V_{RHE}) electrolysis under AM 1.5 G, 100 mW cm^{-2} illumination, 25°C. 0.1 M concentration was used for all standard chemicals shown as references. Glycerol (δ = 62.5, 72.0, ^{13}C NMR signals) used as reference was exposed to 10 h AM 1.5 G, 100 mW cm^{-2} illumination. (DHA: dihydroxyacetone, GALD: glyceraldehyde, GCALD: glycolaldehyde dimers, FA: formic acid, and FMALD: formaldehyde.)

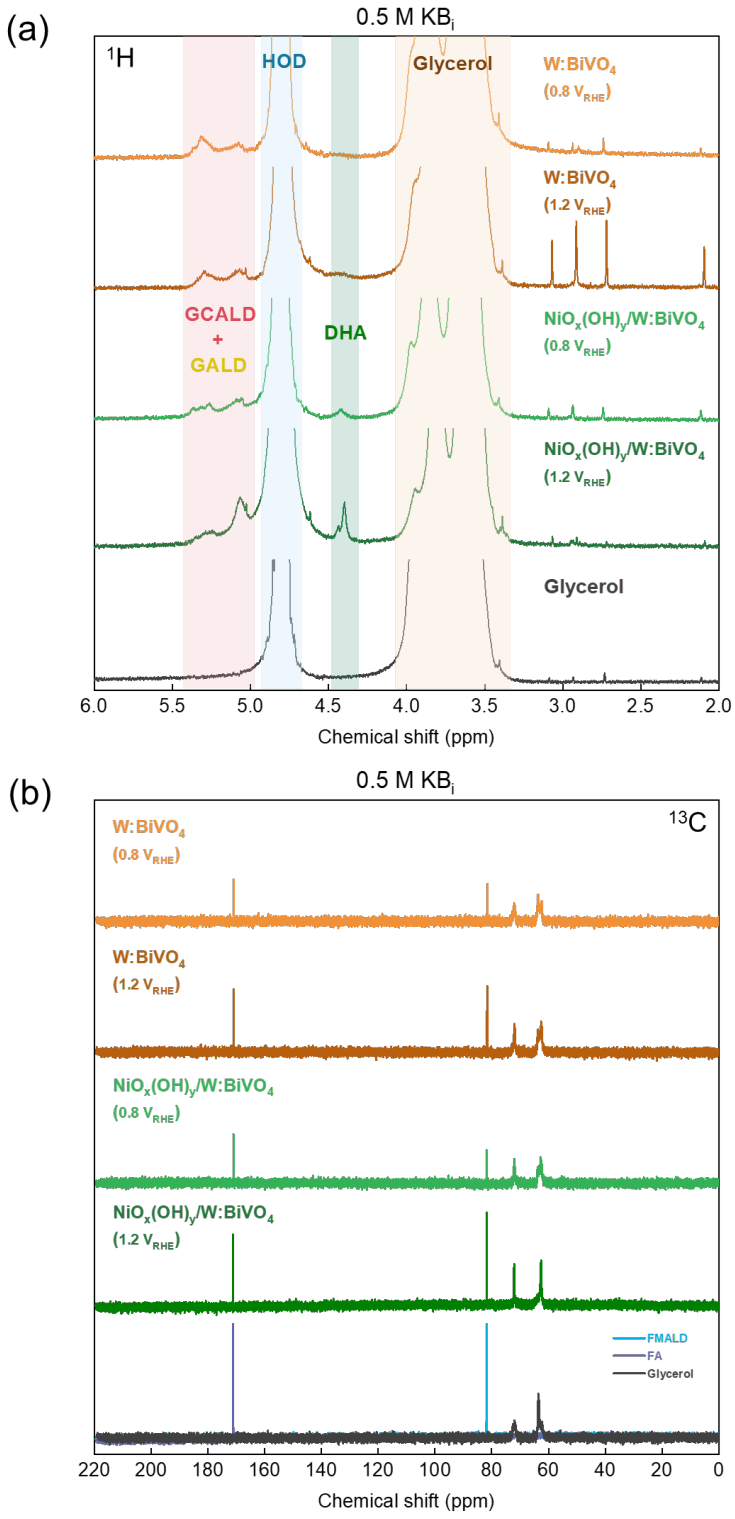

Figure S12 ^{1}H (a) and ^{13}C (b) NMR spectra (400 and 100 MHz, respectively, D_2O) of the reaction mixture of 0.1 M glycerol in 0.5 M KB_i, after 10 h constant potential (0.8 V_{RHE}/1.2 V_{RHE}) electrolysis under AM 1.5 G, 100 mW cm^{-2} illumination, 25°C. 0.1 M concentration was used for all standard chemicals shown as references. Glycerol (δ = 62.6, 72.1, ^{13}C NMR signals) used as reference was exposed to 10 h AM 1.5 G, 100 mW cm^{-2} illumination. (DHA: dihydroxyacetone, GALD: glyceraldehyde, GCALD: glycolaldehyde dimers, FA: formate, and FMALD: formaldehyde.)

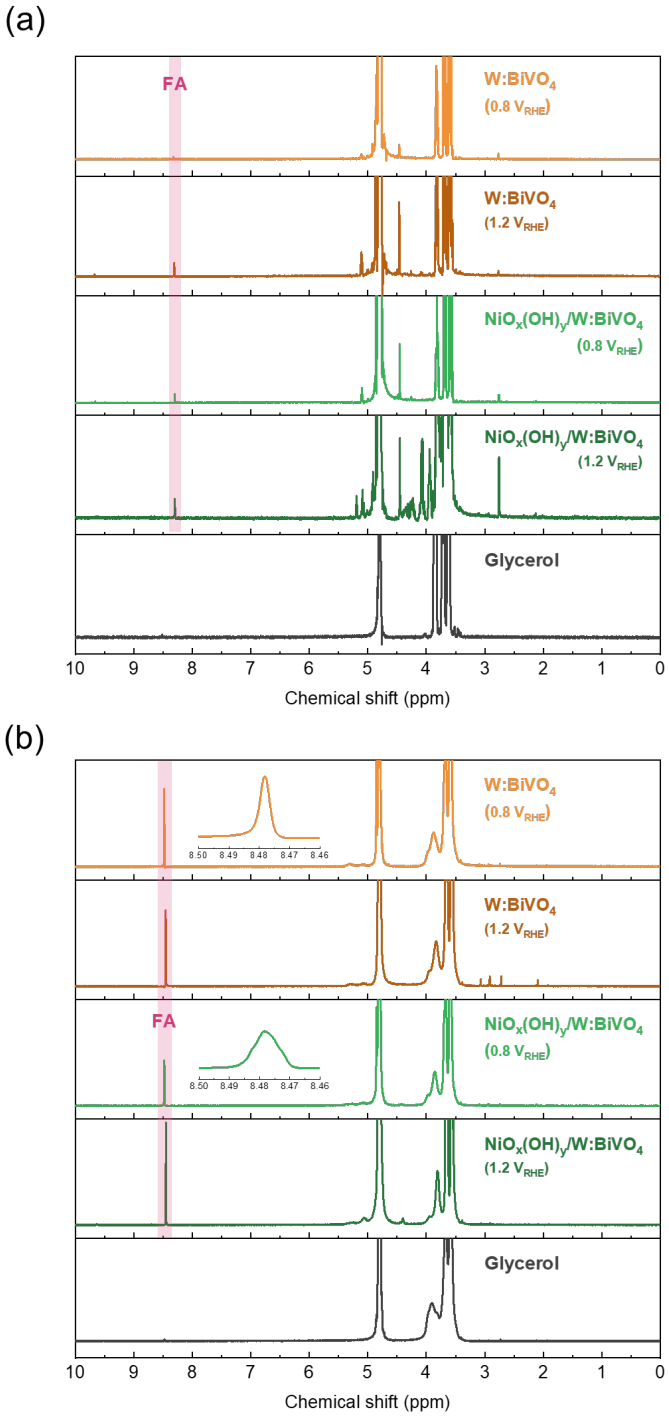

Figure S13 ^{1}H NMR spectra (400 MHz, D_2O) of all targeted PEC conditions in (a) 0.5 M $Na_2SO_{4\ (aq)}$ and (b) 0.5 M KB_i. Insets in (b) show enlarged region of FA peak, showing larger integral area in condition $NiO_x(OH)_y$/W:$BiVO_4$ at 0.8 V_{RHE}. Glycerol denoted here is ^{1}H NMR spectra of 0.1 M glycerol in different media under illumination for 10 h.

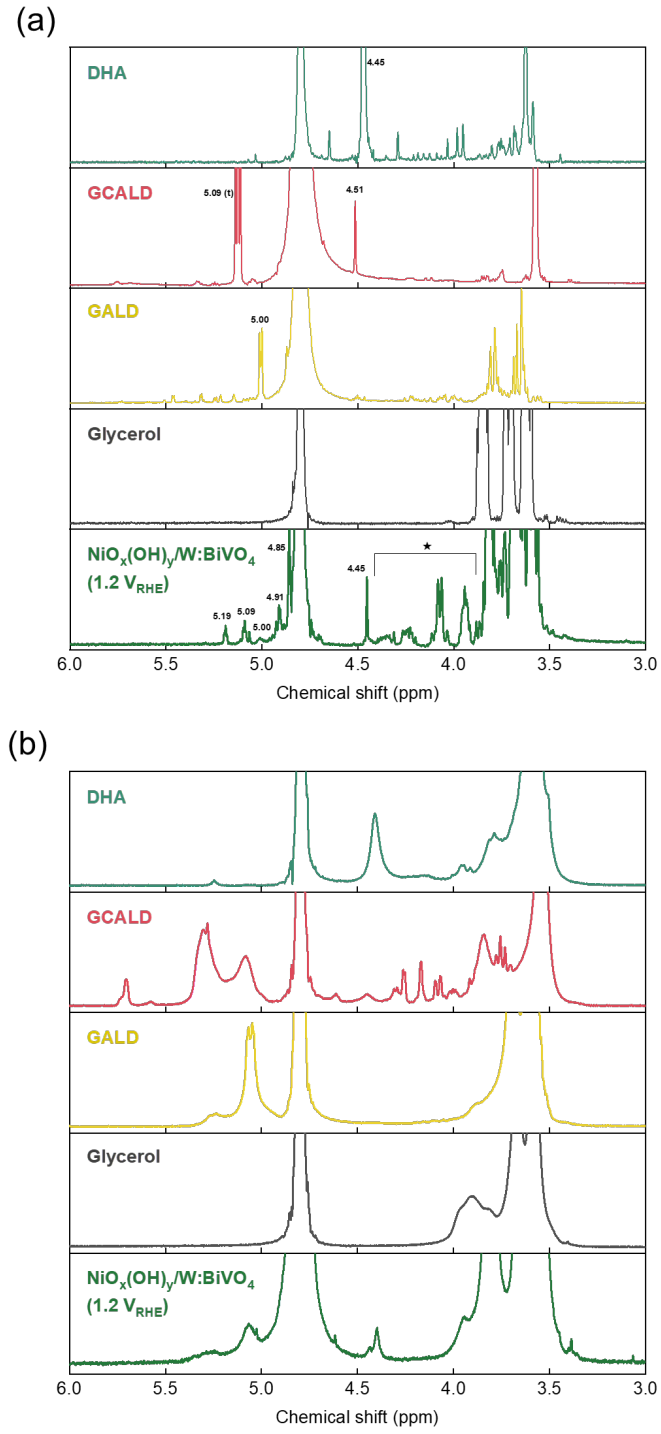

Figure S14 Magnified ^{1}H NMR spectra (400 MHz, D_2O) ranged from 3.0 ppm to 4.0 ppm of DHA, GALD, GCALD, glycerol after 10-h illumination, and GOR condition: $NiO_x(OH)_y$/W:$BiVO_4$ at 1.2 V_{RHE} for 10 h in (a) 0.5 M $Na_2SO_{4\ (aq)}$ and (b) 0.5 M KB_i. All standard chemicals shown here were of 0.1 M concentration. Star sign indicates region with complex signals arising from the mixture of isomers.

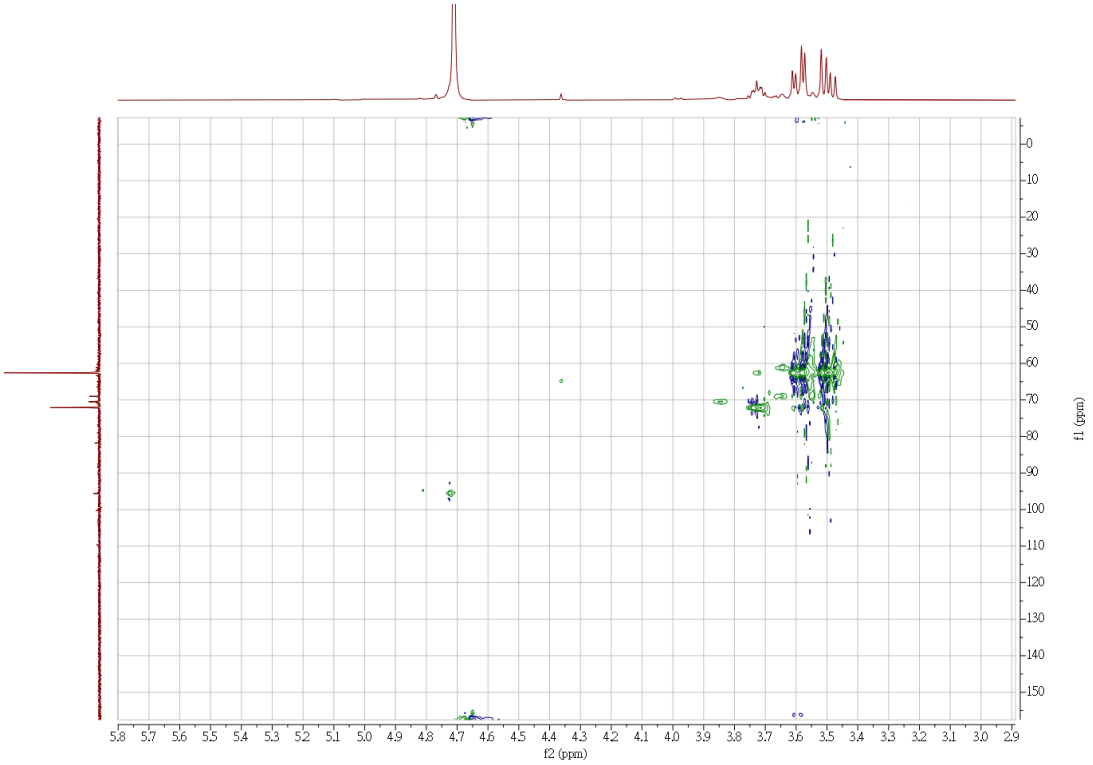

Figure S15 HSQC (400 MHz, D_2O) spectrum of the product mixture after 10-h GOR at 1.2 V_{RHE} using $NiO_x(OH)_y$/W:$BiVO_4$ in 0.5 M Na_2SO_4.

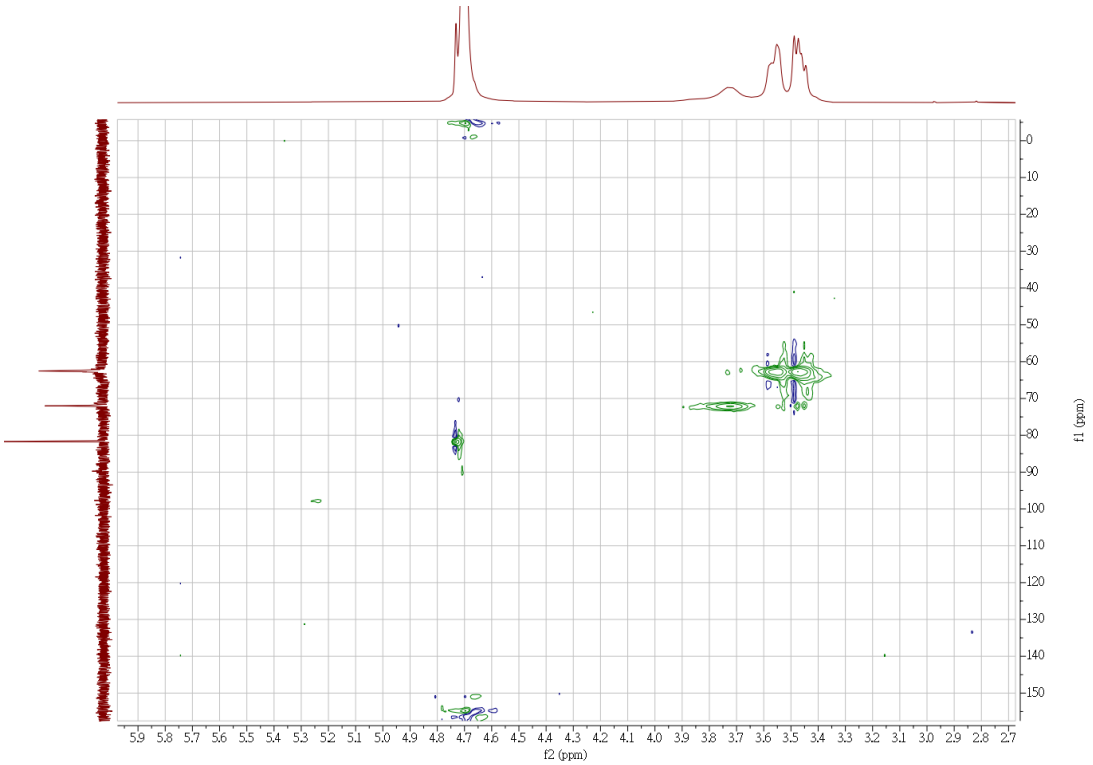

Figure S16 HSQC (400 MHz, D_2O) spectrum of product mixture after 10-h GOR at 1.2 V_{RHE} using $NiO_x(OH)_y$/W:$BiVO_4$ in 0.5 M KB_i.

Table S2 ^{1}H and ^{13}C NMR (400 and 100 MHz, respectively, D_2O) data for C1, C2 and C3 standard products obtained from (photo)electrochemical glycerol oxidation. Only the major (hydrated) isomers are listed (all of these compounds tend to form isomers/oligomers in water; chemical formulas are given for the specific forms detected by NMR). For ^{1}H NMR chemical shifts of glycolaldehyde, glyceraldehyde and dihydroxyacetone, see **Figures S20–S25**.

Compound	Chemical formula	pH	^{1}H NMR chemical shifts (multiplicity)	J_{H-H} coupling values (Hz)	^{13}C NMR chemical shifts / ppm
Glycerol	$(HO)H_2CCH(OH)$-$CH_2(OH)$	7.0	3.58 (dd) 3.68 (dd) 3.82 (ddd)	6.7, 11.7 4.3, 11.7 4.3, 6.7, 10.9	62.5, 72.0
		9.3	3.58 (m) 3.68 (bs) 3.85 (bs)	– – –	62.6, 72.1
			C1 products		
Formic acid	HCOOH	7.0	8.43 (s)	–	169.2
	$HCOO^-$	9.3	8.47 (s)	–	171.1
Formaldehyde	$H_2C(OH)_2$	7.0	4.88 (s)	–	81.7
		9.3	4.84 (s)	–	81.8
			C2 products		
Glycolaldehyde (dimers)	$(HO)H_2CCH(OH)_2$	7.0	3.57 (d) 5.08 (t)	5.0 5.0	64.6, 89.6
		9.3	3.54 (bs) 5.30 (bs)	–	64.5, 68.9, 70.9, 76.1, 81.8, 89.7, 92.7, 102.7
Glyoxylate	$OHCCOO^-$	9.3	5.09 (s) 6.02 (s)	–	88.1, 130.5
Ethylene glycol	$(HO)H_2CCH_2(OH)$	7.0	3.71 (s)	–	62.6
		9.3	3.7 (s)	–	62.6
			C3 products		
Glyceraldehyde	$(HO)_2CCH(OH)CH_2OH$	7.0	3.65 (m) 3.79 (m) 5.00 (d)	– – 4.9	62.05, 74.1, 89.8
		9.3	3.59 (bs) 3.7 (bs) 5.05 (bd)	– – 7.7	62.9, 80.1, 94.2
Dihydroxyacetone	$HOH_2CC(OH)_2CH_2OH$	7.0	3.62 (s)	–	64.9, 95.1

		4.47 (s)		
	9.3	3.6 (bs) 4.41 (bs)	–	64.9, 99.5

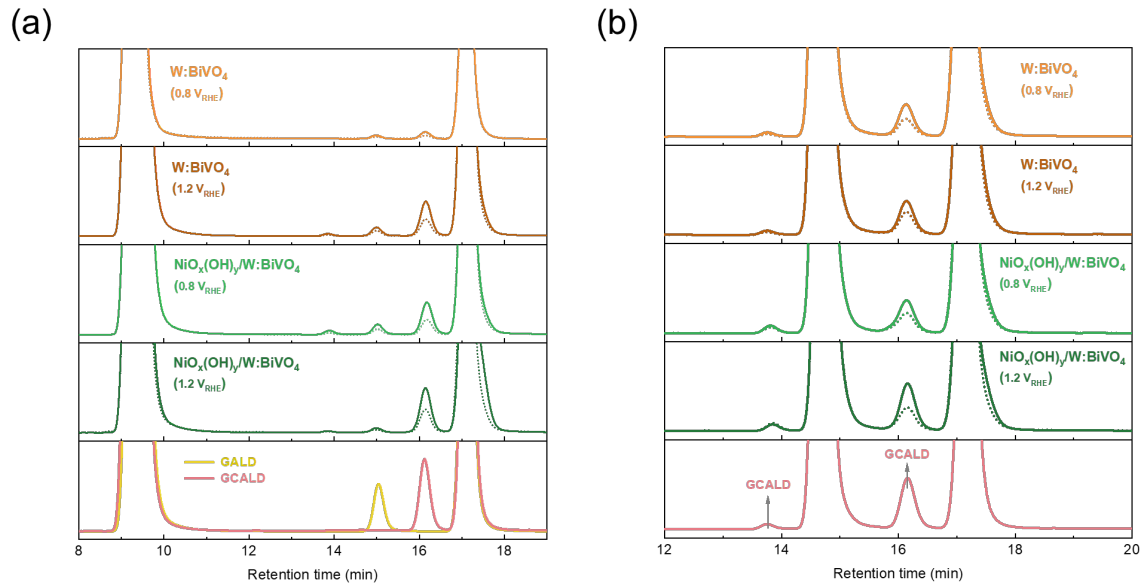

Figure S17 Chromatograms of studied PEC conditions in (a) 0.5 M Na_2SO_4 $_{(aq)}$ and (b) 0.5 M KB_i with addition of 0.1 M glycerol. Peak at retention time 17.1 min belongs to glycerol, while this peak overlaps with some prospective products, e.g. DHA, FA, FMALD. The standard chemicals shown here are all with concentration of 10 mM. HPLC parameters: flow rate = 0.5 ml/min; column temperature is 60 °C.

For GOR in 0.5 M Na_2SO_4 and 0.5 M KB_i, GCALD emerges as two characteristic peaks (13.8 min and 16.2 min) in chromatograms likely accounting for the presence of the two interconverting species of the hydrated glycolaldehyde, as discussed in literature.[3]

In 0.5 M Na_2SO_4, peaks reside at 9.5 min and 17.3 min presenting characteristic peak of electrolyte and glycerol, respectively. In 0.5 M KB_i, these two peaks locate at respective 14.8 min and 17.3 min.

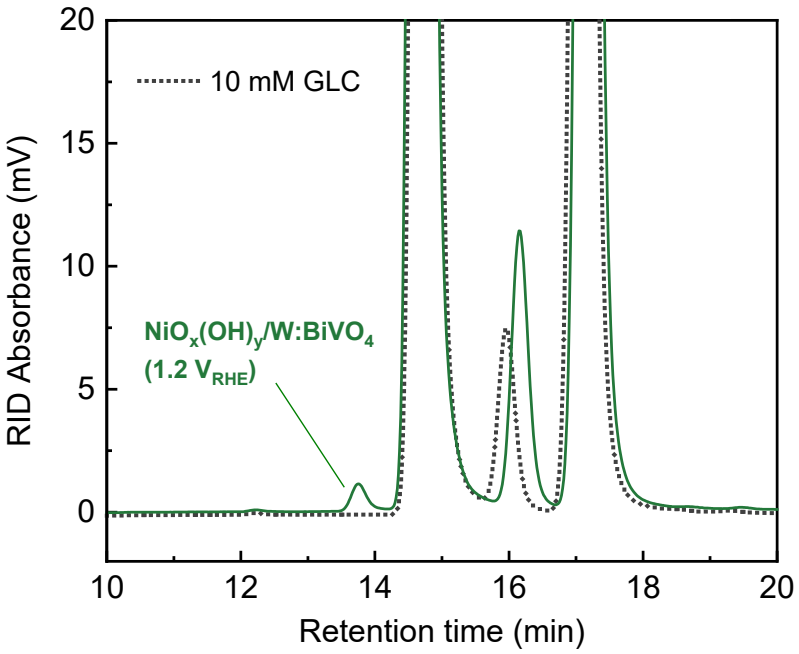

Figure S18 Chromatograms of 10 mM glycolic acid (GLC) in 0.1M glycerol + 0.5 M KB_i and electrolyte after 10-h GOR using $NiO_x(OH)_y$/W:$BiVO_4$ as the photoanode and an applied bias of 1.2 V_{RHE}. The mismatch between the peaks confirms that the generated product is not glycolate.

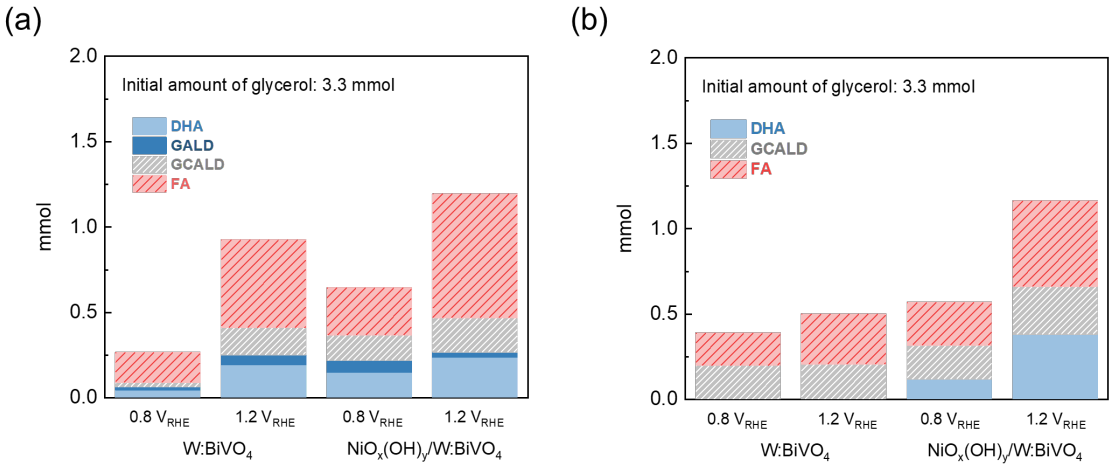

Figure S19 Quantitative product analysis (mmol) after 10 h continuous GOR over W:$BiVO_4$ and $NiO_x(OH)_y$/ W:$BiVO_4$ at different bias in (a) 0.5 M $Na_2SO_{4(aq)}$ and (b) 0.5 M KB_i using HPLC and ^{1}H NMR. Initial concentration of glycerol: 0.1 M. Volume of the cell (anode part) is 0.033 L.

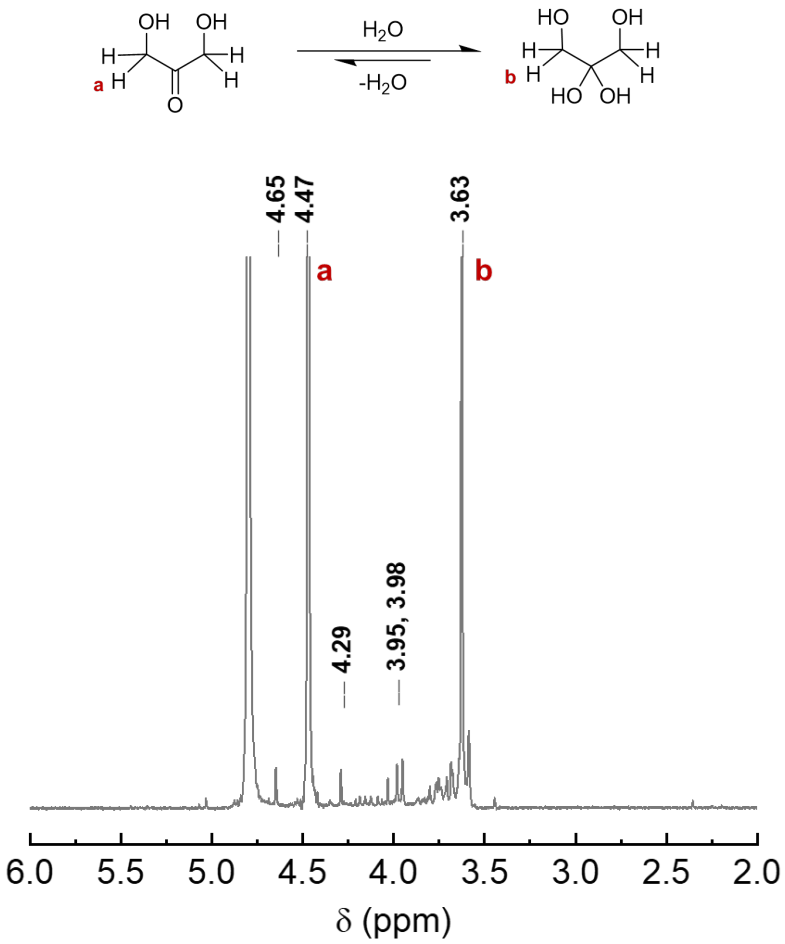

Figure S20 ^{1}H NMR (400 MHz, D_2O) reference spectrum of pure dihydroxyacetone in 0.5 M Na_2SO_4.

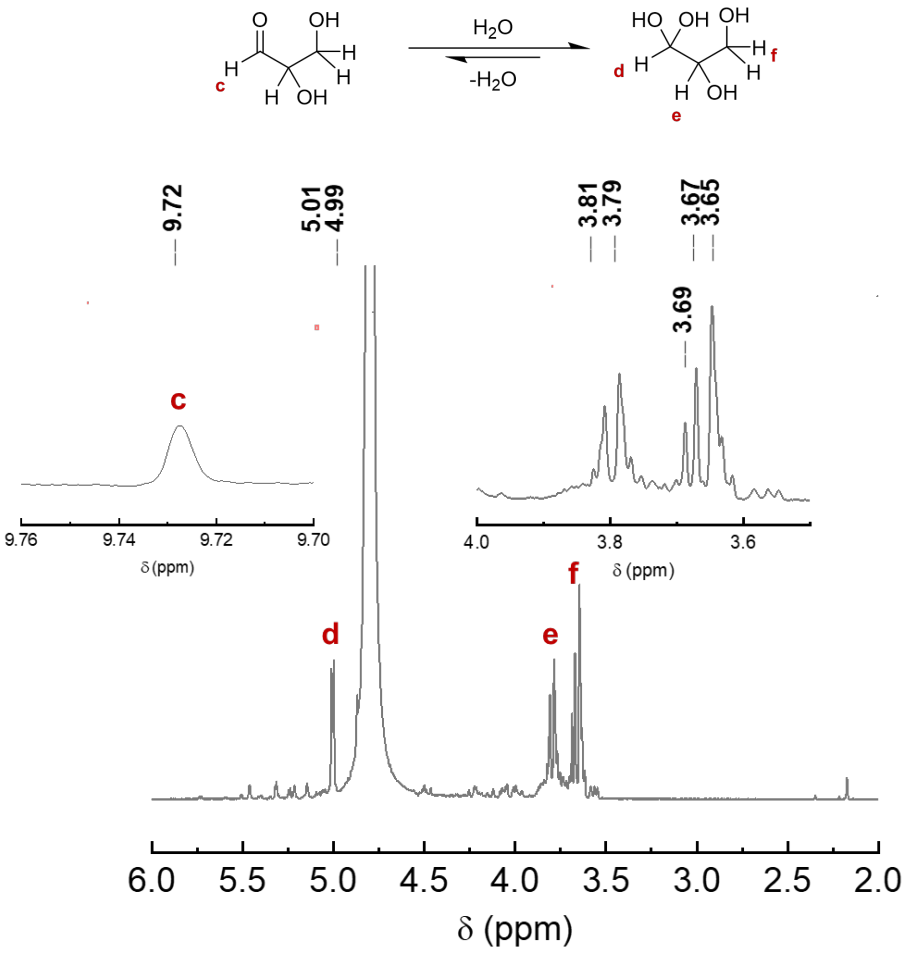

Figure S21 ^{1}H NMR (400 MHz, D_2O) reference spectrum of pure glyceraldehyde dimer in 0.5 M Na_2SO_4. The hydrated form is preferred.

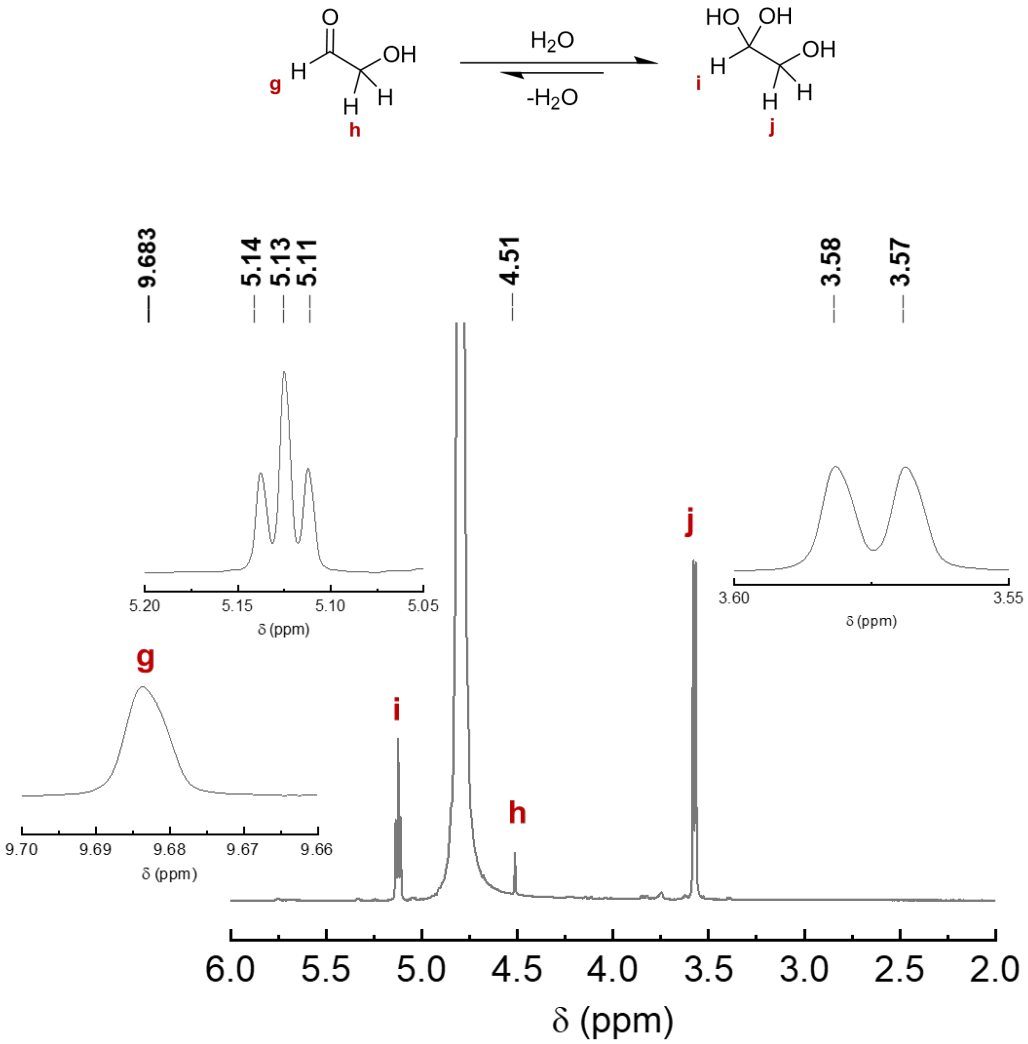

Figure S22 ^{1}H NMR (400 MHz, D_2O) reference spectrum of pure glycolaldehyde dimer in 0.5 M Na_2SO_4. The hydrated form is preferred.

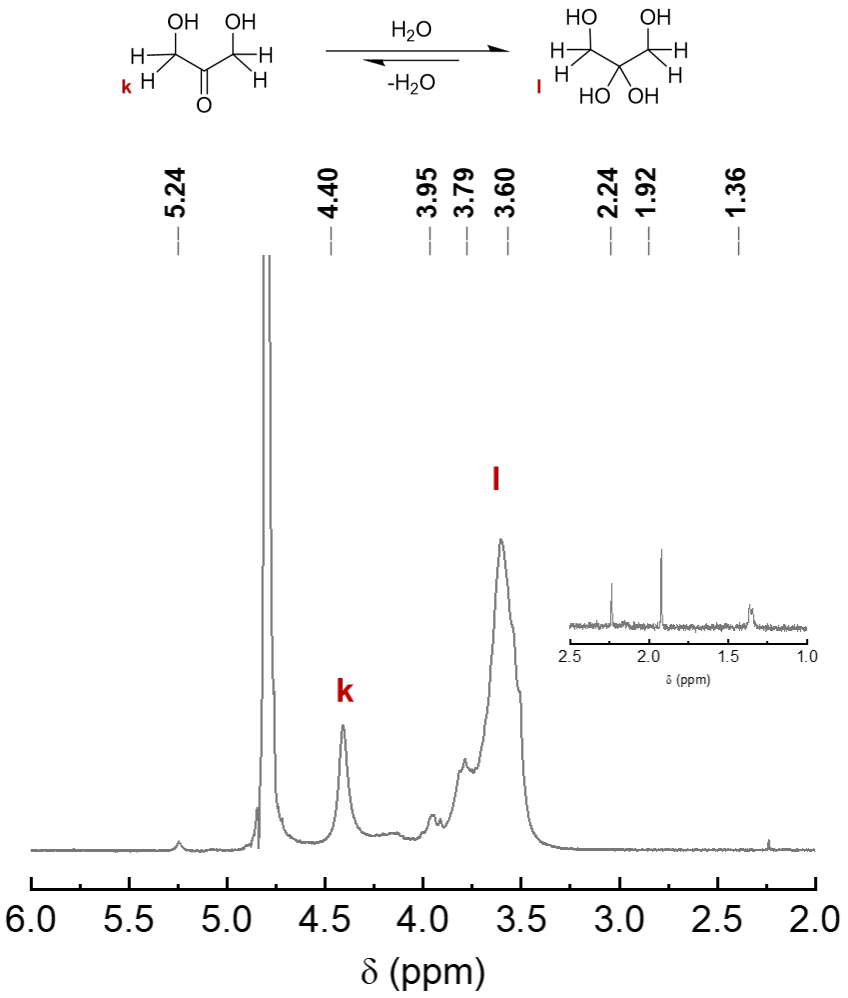

Figure S23 ^{1}H NMR (400 MHz, D_2O) reference spectrum of pure dihydroxyacetone in 0.5 M KB_i.

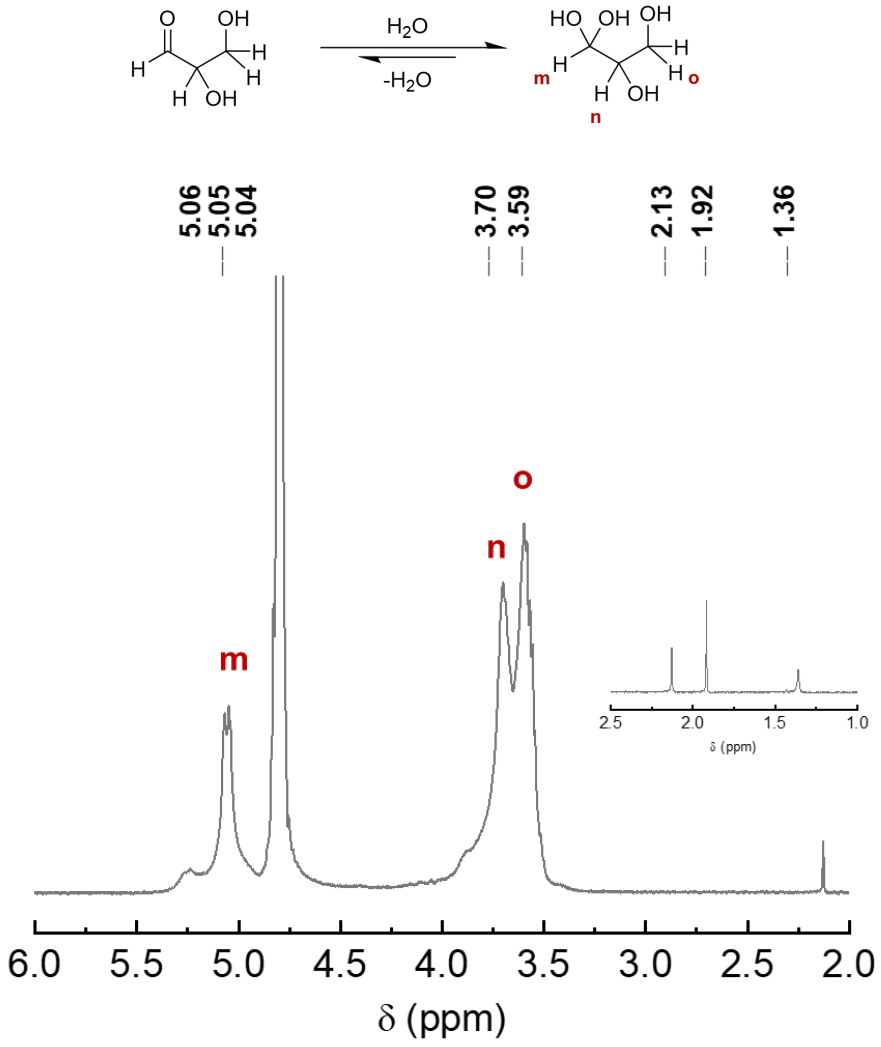

Figure S24 ^{1}H NMR (400 MHz, D_2O) reference spectrum of pure glyceraldehyde dimer in 0.5 M KB_i. The hydrated form is preferred.

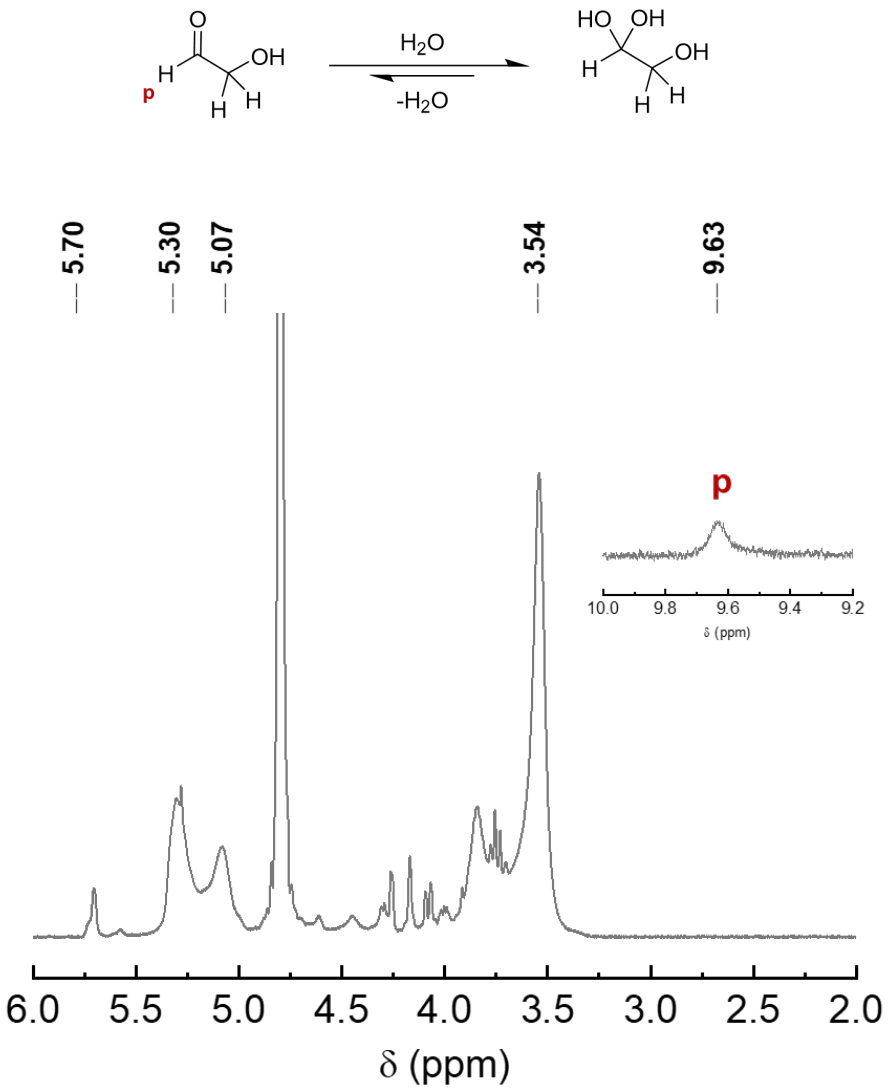

Figure S25 ^{1}H NMR (400 MHz, D_2O) reference spectrum of pure glycolaldehyde dimer in 0.5 M KB_i. The hydrated form is preferred.

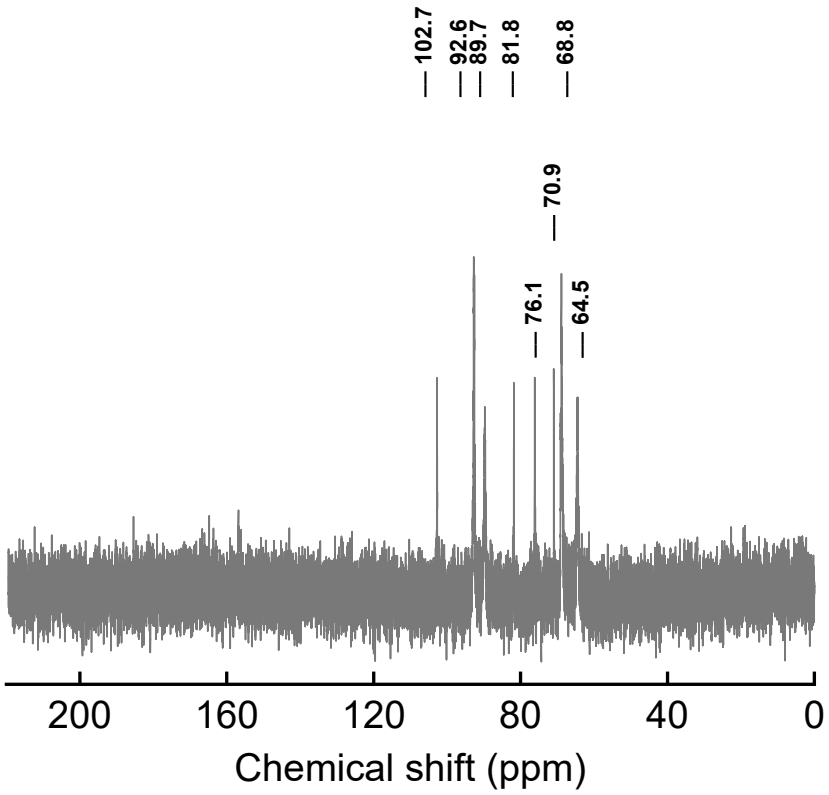

Figure S26 ^{13}C NMR (100 MHz, D_2O) reference spectrum of pure glycolaldehyde dimer in 0.5 M KB_i.

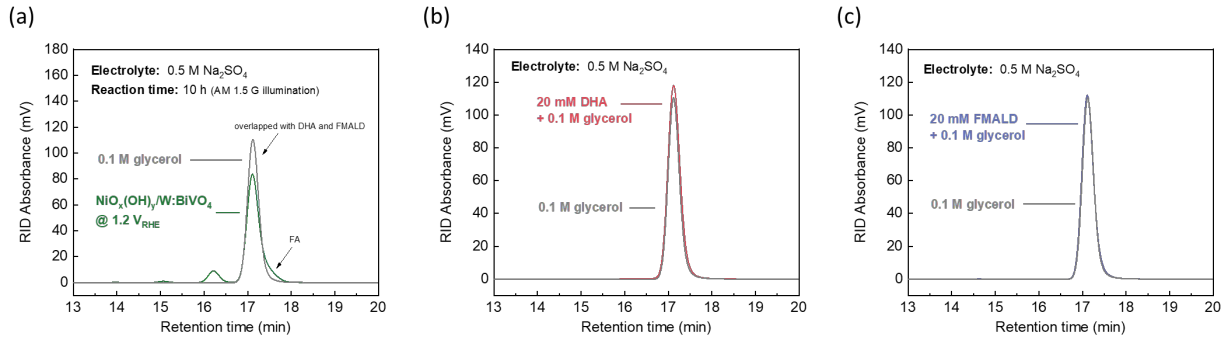

Figure S27 (a) Chromatograms of 0.1 M glycerol and reaction mixtures. Conditions: 10 h chronoamperometry experiment at 1.2 V_{RHE} on $NiO_x(OH)_y$/W:$BiVO_4$ in 0.1 M glycerol and 0.5 M Na_2SO_4. (b) Chromatograms of 0.1 M glycerol and 20 mM DHA in 0.1 M glycerol. (c) Chromatograms of 0.1 M glycerol and 20 mM FMALD in 0.1 M glycerol.

As seen in Figure S27, integral area of the chromatogram peak at the retention time corresponding to glycerol (~ 17 min) decreases by ~ 26 %, matching well the consumption of ~ 35% of glycerol, estimated from the concentration of the reaction products by NMR and HPLC analysis. The discrepancy between HPLC and NMR quantification can be due to the accumulation of DHA and FMALD, whose HPLC peaks overlap with that of glycerol (Figure S26b and S26c).

References

1. K. J. McDonald and K.-S. Choi, *Energy Environ. Sci.*, 2012, **5**, 8553.
2. D. K. Lee and K.-S. Choi, *Nat. Energy*, 2017, **3**, 53-60.
3. V. A. Yaylayan, S. Harty-Majors and A. A. Ismail, *Carbohydr. Res.*, 1998, **309**, 31-38.